International Journal of Scientific Research in Computer Science and Engineering
Research Paper
Vol.5, Issue.3, pp.30-41, June (2017)
E-ISSN: 2320-7639

Accurate Prediction of Fetal Images for measuring growth of Fetus using Genetic Algorithm and Back-Propagation Technique of Neural Network

P.Kaur[1*], G. Singh[2], P. Kaur [3]

[1*] Department of CET, GNDU, Amritsar, India
[2, 3] Department of CS, GNDU, Amritsar, India

[*]*Corresponding Author: prabhpreet.cst@gndu.ac.in*

Available online at: www.isroset.org
Received 17 May 2017, Revised 28th May 2017, Accepted 15th Jun 2017, Online 30th Jun 2017

***Abstract*—** Computer Aided Diagnosis (CAD) plays a crucial role in accurately predicting fetal development recently. In this paper, an automatic fetal development measurement as well as classification technique is explained, the goal is to overcome the limitations of accuracy as well as sensitivity in the existing solution of fetal development diagnosis, firstly, the fetal ultrasound image is auto-preprocessed using novel integrated technique, after which texture features like characteristics, Region of Interest (ROI) , as well as background are extracted, and finally, the features are distinguished among abnormal or normal using neuro-fuzzy classifier. Experimental results of proposed technique shows better accuracy rate of classification of 97 % on the benchmark database images with regard to other existing classification methods .The values of sensitivity, specificity, precision rate, recall, F-measure, are much better than those obtained with the other methods. The use of Accuracy (AUC) of Region of Curve (ROC) as assessment indicators is also done to examine the availability of the feature information and the classification accuracy more clearly. These indicators cross-verify the effectiveness of the proposed method.

***Keywords*—** Ultrasound (US), Artificial Neural Network (ANN), Computer-Aided Diagnostic (CAD), Normal Shrink, Discrete Wavelet Transform (DWT)

I. INTRODUCTION

Ultrasonography is considered to be one of the most powerful techniques for imaging organs and soft tissue structures in human body. It is preferred over other medical imaging methods like Computed Tomography (CT) or Magnetic Resonance Imaging (MRI) because it is: non-invasive, portable, versatile, does not use ionizing radiations and low cost. Despite their obvious advantages, Ultrasound (US) images are contaminated with multiplicative noise called 'speckle' which is one of the major sources of image quality degradation.

Since US images are operator dependent, patient-specific as well as machine specific, that makes appearance of image tightly associated with patient characteristics, the expertise of the clinician in image acquisition, as well as the machine used. Because of the properties of image formation intrinsic to US images, they might get affected by signal dropouts, missing boundaries, artifacts, attenuation, shadows, or speckle, making US essentially the most challenging modalities to operate with. In the medical literature, speckle has been treated as a distracting artifact as it tends to degrade the resolution and the object detectability. Moreover, in US images the speckle noise has a spatial correlation length on each axis, which is same as resolution cell size. This spatial correlation makes the speckle suppression a very difficult and delicate task, hence, a trade-off has to be made between the degree of speckle suppression and feature preservation [21]. Speckle significantly degrades the image quality and hence, makes it more difficult for the observer to discriminate fine detail of the images in diagnostic examinations [22]. Speckle is a form of multiplicative noise, which makes visual interpretation difficult [23]. Image denoising is used to remove the noise while retaining as much as possible the important signal features [24]. The purpose of image denoising is to estimate the presence of noisy data in original image. Image denoising is still remains the challenge for researchers because noise removal introduces artifacts and causes blurring of the images. Protocols are explained to obtain the ideal images while keeping the features of region of interest e.g., shape and structure. Two dimension fetal ultrasound images are commonly utilized to determine the gestational age of the baby, its weight and size, as well as its growth patterns and abnormalities [1]. Normally, size of fetal is determined by employing two dimension ultrasound measurements of head, abdomen, and femur, of about 20 weeks fetal [2] which are then compared to growth charts to distinguish normal and abnormal development. In order to minimize intra- and inter-observer variations, as well as produce better results, automated techniques for fetal biometric measurements are studied [3,4]. This also enhances the efficiency by minimizing the analysis time and different steps required for fetal measurement [5]. Less experienced users are also benefitted from this technique. The automatic examination of US images is challenging, and techniques applied to MRI or CT not compulsorily work with ultrasound images. The automated segmentation techniques earlier introduced in the fetal image area concentrated on utilizing segmentation as a processing step to estimate biometric measurements. Methods providing all fetal biometric measurements employed in clinical practice are limited. Also the healthy fetal changes its shape due to growth and various organs which surround the region of interest create high pose and shape variability for the similar structure of an appealing application of PACS environment together with CAD system in Figure 1.

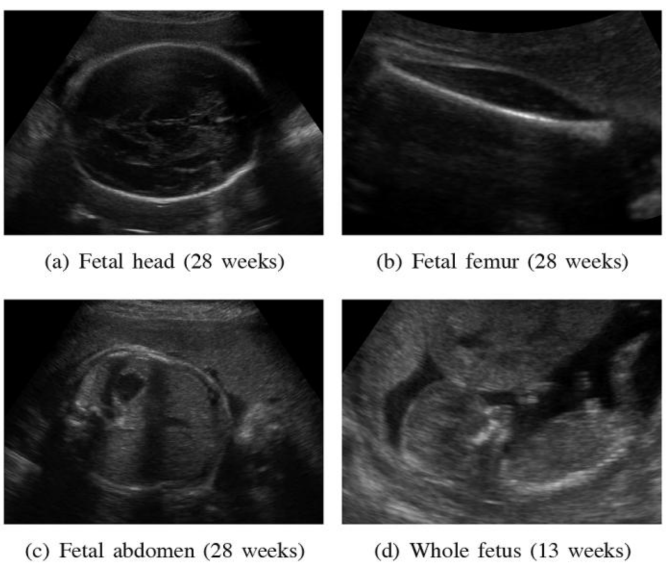

Figure 1: Fetal Ultrasound images of (a) head, (b) femur, (c) abdomen, (d) whole fetus of age 13 weeks.

Previously numerous researchers have focused on the CAD development in multiple fields of medical as in Figure 2. Typically an entire CAD system with regard to fetal examination includes three primary steps discussed in Figure 3: segmentation, feature extraction and classification. Image preprocessing is an essential approach intended for applications based on quantitative analysis. During this phase, the object within the image must be delineated properly. The next procedure is feature extraction for outlining the image characteristics utilizing geometrical and texture feature, intensity, location etc The last approach is classification in which different classifiers, like k-NNs, random forest, Support Vector Machine(SVM) or Artificial Neural Network(ANN), is used to distinguish normal samples from abnormal. In this paper, the development of CAD system for fetal development examination is carried out. This work is directed at automatically locating abnormal signs of a diffuse textural nature found within fetal development. The primary contributions include the segmentation of the fetus picture based on multiple parameters, together with histogram and co-occurrence matrices in order to obtain characteristics from each and every sub image, the utility of neuro-fuzzy as a part of classification scheme into normal and abnormal cases. The scheme is initialized with the fetus image preprocessing using cropping and edge detection techniques. Then background subtraction is performed to eliminate the abnormalities from the fetus preprocessed images. On the original and processed images, the histogram, GLCM, GLRLM and the rotation invariant moments features are computed from each and every region. Depending on the features determined, neuro-fuzzy using genetic algorithm is applied as a classifier to acquire the final classification.

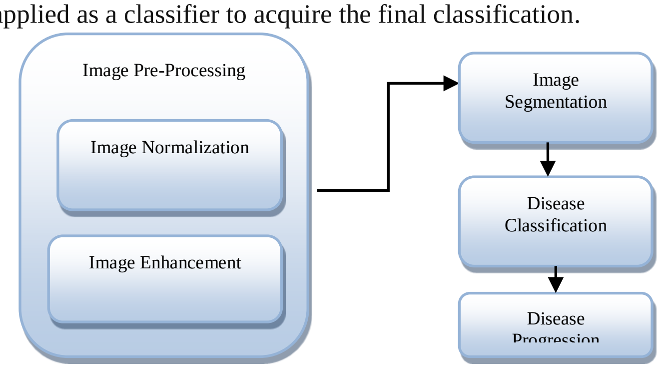

Figure 2: General Framework of CAD

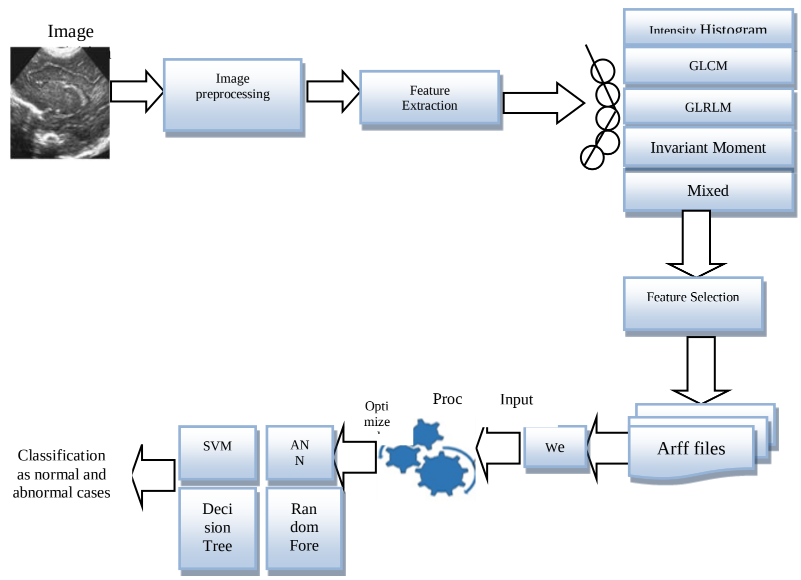

Figure 3: Working of CAD System

The rest of the paper is organized as follow: Section II mentions the state-of-art techniques in the form of related work done in data mining. Section III gives details of various data mining techniques. Section IV explains about the proposed method with workflow. Section V deals with Results and Discussions and Conclusion is discussed in Section VI and the references are mentioned in the last section.

II. STATE-OF-ART TECHNIQUES

Amongst the techniques commonly utilized in the area of texture-based depiction of the growth factors, presently there exists the Grey Levels Co-occurrence Matrix (GLCM), the Run-Length Matrix parameters [6], the Wavelet transform [7], together with the k-nearest-neighbor classifiers, fractal-based techniques [8], Bayesian classifiers [6], ANN, Fisher Linear Discriminants [8], SVM [7]. The Wavelet transform was applied in an effort to examine the values of the textural parameters at multiple resolutions, for distinguishing malignant or benign liver tumors in US images [7].The fractal based techniques are utilized [8] to differentiate the salivary gland tumors in the US images. The combinations of classifiers were analyzed so as to differentiate the brain tumors in MRI in [9]. With regard to execution of the multiclass classification methods, in [10] the authors put into practice multiclass recognition based on SVM so as to differentiate various cancer types by utilizing genes expressions as an input attribute. A voting plan was applied, in order to integrate classifiers having different behaviors: decision trees, linear discriminants, and k-NN. In order to improve the recognition and segmentation of the bronchial tumors, multiple classifier combo strategies were also compared in [11]. On the other hand, no thorough research has been carried out with the existing classification methods to examine the growth of fetal.

III. METHODS

A. Dataset

The experiment has been performed on the online benchmark dataset available on http://www3.medical.philips.com shown in the Figure 4.

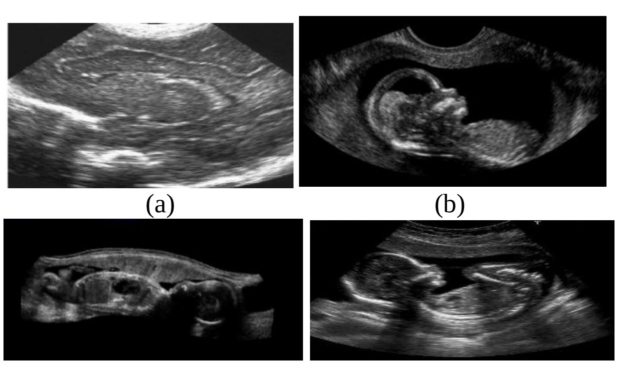

Figure 4: Database images (a) US_orig (b) us1 (c) us2 (d) us3

B. Image Pre-processing

The image preprocessing methods are used to get the efficient results for further analysis. We applied three image preprocessing techniques such as Wavelet based Denoising, Homomorphic NormalShrink Filtering Technique based on 2-DWT (Two Discrete Wavelet Transform) and then enhanced image cropping applied. Cropping eliminates the undesirable parts of the image usually peripheral to the area of interest. The result is passed as an input to the feature extraction step.

- **Wavelet based Denoising**

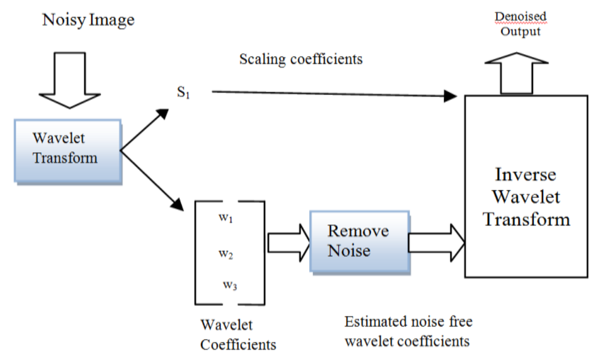

Figure 5: Wavelet Based Denoising

The steps explaining the Wavelet based Denosing of Medical US fetal images as in Figure 5:

a) Perform a suitable wavelet transform of the noisy data; (the wavelet basis may be chosen based on various factors including computational burden, and ability to compress the L2 energy of the signal into a very few, very large coefficients).

b) Perform a soft thresholding of the wavelet coefficients where the threshold depends on the noise variance; (when the wavelet bases are chosen as in step 1, thresholding kills the effect of the noise without killing the effect of the signal).

c) The coefficients obtained from step 2 are then padded with zeros to produce legitimate wavelet transform and this is inverted to obtain the signal estimate and the denoised output image [24].

- **Implementation of 2D Wavelet Transform**

The Discrete Wavelet Transform is identical to a hierarchical sub-band system where the sub- bands are logarithmically spaced in frequency and represent octave-band decomposition. By applying DWT, the image is actually divided i.e., decomposed into four sub-bands and critically sub-sampled as shown in Figure 6:

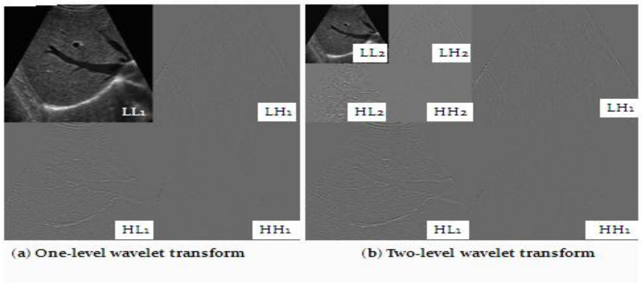

Figure 6: Working of 2DWT US fetus Image

These sub-bands labeled LH1, HL1 and HH1 represent the finest scale wavelet coefficients i.e., detail images while the sub-band LL1 corresponds to coarse level coefficients i.e., approximation image. To obtain the next coarse level of wavelet coefficients, the sub-band LL1 alone is further decomposed and critically sampled using similar filter bank.

- **Wavelet Based Homomorphic NormalShrink Technique**

In the homomorphic techniques, the wavelet filtering is applied to the image-logarithm followed by an exponential operation. Zong et al. proposed a homomorphic wavelet shrinkage technique to separate the speckle noise from the original image [23].

NormalShrink is an adaptive threshold estimation method for image denoising in the wavelet domain based on the generalized Gaussian distribution (GGD) modelling of sub-band coefficients. It is computationally more efficient and adaptive because the parameters required for estimating the threshold depend on sub-band data.

The steps of NormalShrink for image denoising are as follows:

1) Take the logarithmic transform of the speckled image.

2) Perform multiscale decomposition of the image corrupted by Gaussian noise using wavelet transform.

3) Estimate the noise variance from subband HH1 using formula:

$$\hat{\sigma}^2 = \left[\frac{median(|Y_{ij}|)}{0.6745}\right]^2, \ 'Y_{ij}' \in subband\ HH_1 \text{ HH1} \tag{1}$$

4) For each level, compute the scale parameter ‘β’ using the equation:

$$\beta = \sqrt{\log\left(\frac{L_k}{J}\right)} \tag{2}$$

5) For each sub-band (except the low pass residual):

a) Compute the standard deviation $'\sigma_y'$

b) Compute threshold T_N using equation

$$T_N = \frac{\beta\,\hat{\sigma}^2}{\hat{\sigma}_y} \tag{3}$$

c) Apply soft thresholding to the noisy coefficients.

6) Invert the multiscale decomposition to reconstruct denoised image $\hat{f}$

7) Take the exponential of the reconstructed image obtained from step 6 [24].

The image preprocessing work flow is analyzed in the Figure 7 which include original benchmark image, ROI (Region of Interest) and the enhanced Normal Shrink Wavelet based filtered image.

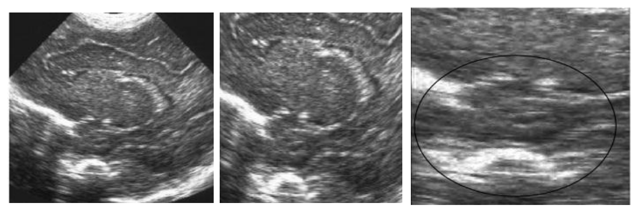

(a) (b) (c)

Figure 7: Workflow of image preprocessing step, (a) original ultrasound image, (b) ROI image , (c) Enhanced NormalShrink Wavelet Cropped Image

C. Feature Extraction

Feature extraction is used to discover efficient measures so as to present the abnormalities appeared within medical image. After pre-processing of the images, that signifies the data-cleaning phase, attributes related to the classification are taken from the cleaned images using techniques explained as follows.

- **Intensity Histogram (IH) Features**

Intensity Histogram texture measures tend to be computed through original image values and it comes within the category of first-order statistics. They don’t take into account connections with neighborhood pixel. Features obtained using this strategy is listed in Table 1 along with their equations [13].

Table1: Features of Intensity Histogram

S.No	Name	Equation
1	Mean(μ)	$\mu = \sum_{s=0}^{N-1} sp(s)$
2	Energy(E)	$E = \sum_{s=0}^{N-1} p(s)^2$
3	Variance(σ2)	$(\sigma_2) = \sum_{s=0}^{N-1} (s-\mu)^2 p(s)$

4	Entropy	$H = \sum_{s=0}^{N-1} p(s) log_2 p(s)$
5	Skewness	$\mu_3 = \sigma^{-3} \sum_{s=0}^{N-1} (s-\mu)^3 p(s)$
6	Kurtosis	$\mu_4 = \sigma^{-4} \sum_{s=0}^{N-1} (s-\mu)^4 p(s) - 3$

- **Gray Level Co-occurrence Matrix (GLCM)**

GLCM is also referred as "Spatial Dependency". It is one of the most commonly used mathematical tools for extracting information about texture from images. This technique always concentrates on the pixel intensity level of the neighboring pixel. GLCM always accounts for the particular position of the pixel comparative to other pixel. This is a simple tabulation 2, which indicates how often the distinct combinations of pixel brightness values forms in medical images [14, 15].

Table 2: Features of GLCM

S.No	Name	Equation
1	Mean(μx,μy)	$\mu_x = \sum_{\hat{\imath}} \sum_{\hat{\jmath}} \hat{\imath}. p_x(\hat{\imath},\hat{\jmath})$ $\mu_y = \sum_{\hat{\imath}} \sum_{\hat{\jmath}} \hat{\jmath}. p_x(\hat{\imath},\hat{\jmath})$
2	Standard Deviations	$\sigma_x = \sum_{\hat{\imath}} \sum_{\hat{\jmath}} (\hat{\imath} - \mu_x)^2 . p_x(\hat{\imath},\hat{\jmath})$ $\sigma_y = \sum_{\hat{\imath}} \sum_{\hat{\jmath}} (\hat{\imath} - \mu y)^2 . p_x(\hat{\imath},\hat{\jmath})$
3.	Autocorrelation	$f_1 = \sum_{\hat{\imath}} \sum_{\hat{\jmath}} (\hat{\imath}\hat{\jmath}). p_x(\hat{\imath},\hat{\jmath})$
4	Contrast	$f_2 = \sum_{n=0}^{N^{g}-1} n^2 \{ \sum_{\hat{\imath}=1}^{Ng} \sum_{\hat{\jmath}=1}^{NG} p_x(\hat{\imath},\hat{\jmath}) \mid \lvert \hat{\imath} - \hat{\jmath} \rvert = n \}$
5	Correlation	$f_3 = \frac{[\sum_{\mathrm{i}} \sum \mathrm{j} (\hat{\imath}\hat{\jmath}) p_x(\hat{\imath},\hat{\jmath}) - \mu x \mu y]}{\sigma x \sigma y}$
6	Cluster Shade	$f_5 = \sum_{\hat{\imath}} \sum_{\hat{\jmath}} (\hat{\imath} + \hat{\jmath} - \mu x - \mu y)^3 p_x(\hat{\imath},\hat{\jmath})$
7	Dissimilarity	$f_6 = \sum_{\hat{\imath}} \sum_{\hat{\jmath}} \lvert \hat{\imath} - l \rvert . p_x(\hat{\imath},\hat{\jmath})$
8	Energy	$f_7 = \sum_{\hat{\imath}} \sum_{\hat{\jmath}} p_x(\hat{\imath},\hat{\jmath})^{\,2}$
9	Entropy	$f_8 = \sum_{\hat{\imath}} \sum_{\hat{\jmath}} p_x(\hat{\imath},\hat{\jmath}) log(p_x(\hat{\imath},\hat{\jmath}))$
10	Homogenecity	$f_9 = \sum_{\hat{\imath}} \sum_{\hat{\jmath}} \frac{1}{1 + (\hat{\imath} + \hat{\jmath})^2} p_x(\hat{\imath},\hat{\jmath})$
11	Inverse Difference	Same as homogenecity

- **Gray Level Run Length Matrix (GLRLM)**

It is a matrix through which features related to texture analysis can be extracted. For any given 2D image, GLRLM is basically a 2D matrix within which component "p(k,l)" provides total number of consecutives operations of length "l" at grey level "k". Here "M" symbolizes maximum run length (run length is considered to be a number of neighboring pixels which possess same grey level intensity in a specific direction). Table 3 represents the features extracted by GLRLM [16].

Table 3: Features of GLRLM

S.No	Name	Equation
1.	Gray level run length pixel number matrix	$Pp_x(\hat{\imath},\hat{\jmath}) = p_x(\hat{\imath},\hat{\jmath}).\hat{\jmath}$
2	Gray level run number vector	$Pg(\hat{\imath}) = \sum_{\hat{\jmath}=1}^{N} p_x(\hat{\imath},\hat{\jmath})$
3	Run length run number matrix	$Pg(\hat{\imath}) = \sum_{\hat{\jmath}=1}^{N} p_x(\hat{\imath},\hat{\jmath})$
4	Short run emphasis[SRE]	$\boldsymbol{f}_1 = \mathbf{1} / \boldsymbol{n}_{\mathrm{r}} \sum_{\hat{\imath}=1}^{M} \sum_{\hat{\jmath}=1}^{N} \frac{p_x(\hat{\imath},\hat{\jmath})}{\hat{\jmath}^2} = \mathbf{1}/\boldsymbol{n}_{\mathrm{r}} \sum_{\hat{\jmath}=1}^{N} \frac{\boldsymbol{p}_{\mathrm{r}}(\hat{\imath})}{\hat{\jmath}^2}$
5	Long run emphasis[LRE]	$\boldsymbol{f}_2 = \mathbf{1} / \boldsymbol{n}_{\mathrm{r}} \sum_{\hat{\imath}=1}^{M} \sum_{v=1}^{N} (p_x(\hat{\imath},\hat{\jmath}).\hat{\jmath}^2) = \mathbf{1}/\boldsymbol{n}_{\mathrm{r}} \sum_{\hat{\jmath}=1}^{N} \boldsymbol{p}_{\mathrm{r}}(\hat{\jmath}).\hat{\jmath}^2$

6	Gray level non-uniformity[GLN]	$\boldsymbol{f}_3 = \mathbf{1}/\boldsymbol{n}_{\mathrm{r}} \sum_{\hat{\imath}=\mathbf{1}}^{\boldsymbol{M}} \left(\sum_{\hat{\jmath}=\mathbf{1}}^{\boldsymbol{N}} (p_x(\hat{\imath},\hat{\jmath}))^2 \right) = \mathbf{1}/\boldsymbol{n}_{\mathrm{r}} \sum_{\hat{\jmath}=\mathbf{1}}^{\boldsymbol{N}} \boldsymbol{Pg}(\hat{\imath})^{\mathbf{2}}$
7	Run length non-uniformity[RLN]	$\boldsymbol{f}_4 = \mathbf{1}/\boldsymbol{n}_{\mathrm{r}} \sum_{\hat{\imath}=\mathbf{1}}^{\boldsymbol{M}} \left(\sum_{\hat{\jmath}=\mathbf{1}}^{\boldsymbol{N}} (p_x(\hat{\imath},\hat{\jmath}))^2 \right) = \mathbf{1}/\boldsymbol{n}_{\mathrm{r}} \sum_{\hat{\jmath}=\mathbf{1}}^{\boldsymbol{N}} \boldsymbol{P}_{\mathrm{r}}(\hat{\imath})^{\mathbf{2}}$

- **Rotation Invariant Moments (IM)**

The concept of making use of moments inside shape recognition became popular around 1962 when Hu utilized algebraic invariants in order to discover a set of invariants. Hu's seven moment invariants are usually invariant in the form of translation, alterations in scale as well as rotation [16, 17]. Hence it explains the image regardless of its location, size as well as rotation. The moment variants are usually specified interims of normalized moments [18].

D. Feature Selection

All features were extracted from image and the resultant data contains many redundant or irrelevant features. Features selection technique is used to remove those redundant and irrelevant features and to find the significant features, which are useful in further analysis. Feature Selection was performed using WEKA [19] software of Version 3.6.9. WEKA is compatible with and recognizes only '.arff' data files. Therefore '.arff' file was generated which contains the value of features, that were extracted (including both normal as well as abnormal). In feature extraction process, total 16 features were extracted from each image but whole of these features cannot be supplied to the neural network because the number of features is high. Although each feature is important in classification only few of these features are very significant in classifying and identification of the disease conditions. Therefore instead of using all of these features as input, only those features, which have high significance, were selected.

E. Classifier

In CAD system classification is essential among different domains, and its performance relies upon the effective performance of different characteristics and the classifier selection. We can commonly utilize Machine learning techniques in the field of medical imaging, computer vision, pattern recognition, etc. Here ANN has been employed for diagnosis of fetal development and acquires the substantial classification accuracy. But we presume that ANN has definitely not revealed its advantage; therefore in our work, we enhance artificial neural network with fuzzy logic and compare the classification results with ANN.

- **ANN**

A group of artificial neurons that are interconnected which utilizes mathematical or perhaps computational models meant for processing of information based upon linked strategy is called as neural network. ANN is computational model that have the ability to map any kind of non-linear functional relationship in between an input and an output to expected accuracy. These contain many processing units known as neurons or perhaps nodes and vary amongst one another in exactly how these are linked information processing as well as in the level of learning protocols used. Multi-layer neural network are probably the most famous and straight-forward neural network. Particularly the neurons of the multi-layer feed forward NN are structured as 3 layers: in first layer the input nodes receives information from the outer world through data file in the second layer the intermediate neurons found in several hidden layers, enable non-linearity in the data processing, the third layer i.e output layer is actually utilized to give solution for any provided range of input values. In a fully connected ANN, every neuron inside a particular layer is actually linked to every neuron in the next layer by means of an associated weight "w(i,j)". MLP is commonly used like a classifier within the recognition involving patterns [19]. A significant problem that comes across MLP is its back propagation algorithm that utilizes a very long time throughout the training. The second issue is the network structure, i.e. cannot find any rule that enables a person to find the essential structure from a given application or training set. The Figure 8 explains the working of ANN as a classifier.

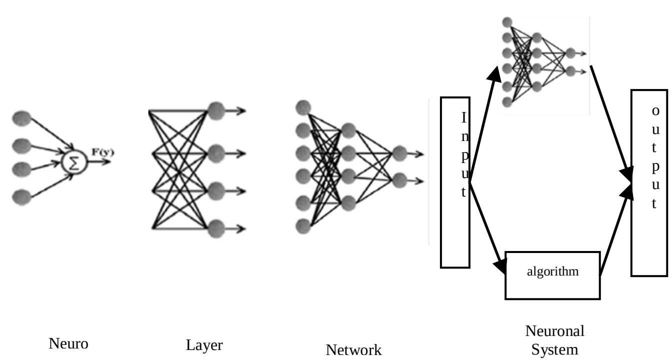

Figure 8: A schematic diagram for a system based on ANN

- **Neuro-Fuzzy**

Integration of ANN with FIS have attached the growing attention of researchers in numerous scientific as well as engineering fields because of increasing necessity of smart systems to resolve the real life issues. ANN learns from scratch through simply changing the interconnections among layers. In case we have knowledge conveyed within linguistic rules, it will be easy to construct FIS, or in case indicate the fuzzy operators, fuzzy sets, along with knowledge base. Likewise for building an ANN for an application the consumer must indicate the design as well as learning algorithm. The disadvantages associated with these methods appear complementary and hence it is obvious to think about developing an integrated system merging both the techniques. Though the ability to learn is a benefit of FIS, the creation of linguistic rule is a benefit of ANN.

Neuro-fuzzy hybridization generates a hybrid smart system which synergizes these both methods by blending the human like reasoning form of fuzzy systems with the learning and connectionist architecture of neural networks. Neuro-fuzzy hybridization is referred as fuzzy neural network (FNN) or neuro-fuzzy system (NFS). NFS includes the human like reasoning form of fuzzy systems by using fuzzy sets and a linguistic design composed of a set of IF-THEN fuzzy rules. The key strength of neuro-fuzzy systems is the universal approximates quality having capability to solicit interpretable IF-THEN rules. The effectiveness of neuro-fuzzy systems consists of two contradictory needs within fuzzy modeling: interpretability versus accuracy among which only one prevails. The neuro-fuzzy within fuzzy modeling study discipline is split among two areas: the Mamdani model, which is a linguistic fuzzy model centered on interpretability and the Takagi-Sugeno-Kang(TSK) model, which is a precise fuzzy model centered on accuracy.

IV. PROBLEM FORMULATION

In this study, the acquisition of normal and abnormal fetal images is considered. Using MATLAB along with “image processing toolbox” these images are then subjected to three different image preprocessing techniques, namely, “denoising”, “discrete wavelet transform”, and “Homomorphic NormalShrink Filtering Technique”, to obtain the region of interest from the acquired images. After image preprocessing, texture features like GLCM were extracted from the processed ultrasound images to compute the texture features. The features extracted from were further processed utilizing “feature selection” method to obtain most significant and optimal features which depict the fetal characteristics. WEKA software was utilized within the feature selection phase to provide the selected significant features. These optimal features then act as an input to the neuro-fuzzy network for classification. Neuro fuzzy using genetic algorithm, was employed for classifying the normal and abnormal fetal characteristics and also to determine which feature classifier is best for classification. The performance of the neuro-fuzzy based classifier was determined using “confusion matrix” and “receiver operating characteristic (ROC)” curve analysis. Figure 9 explains the proposed Methodology. Figure 10 explains the workflow of the proposed methodology. Figure 11 explains the training of the neuro-fuzzy model and Figure 12 explains the testing phase of the neuro-fuzzy proposed model.

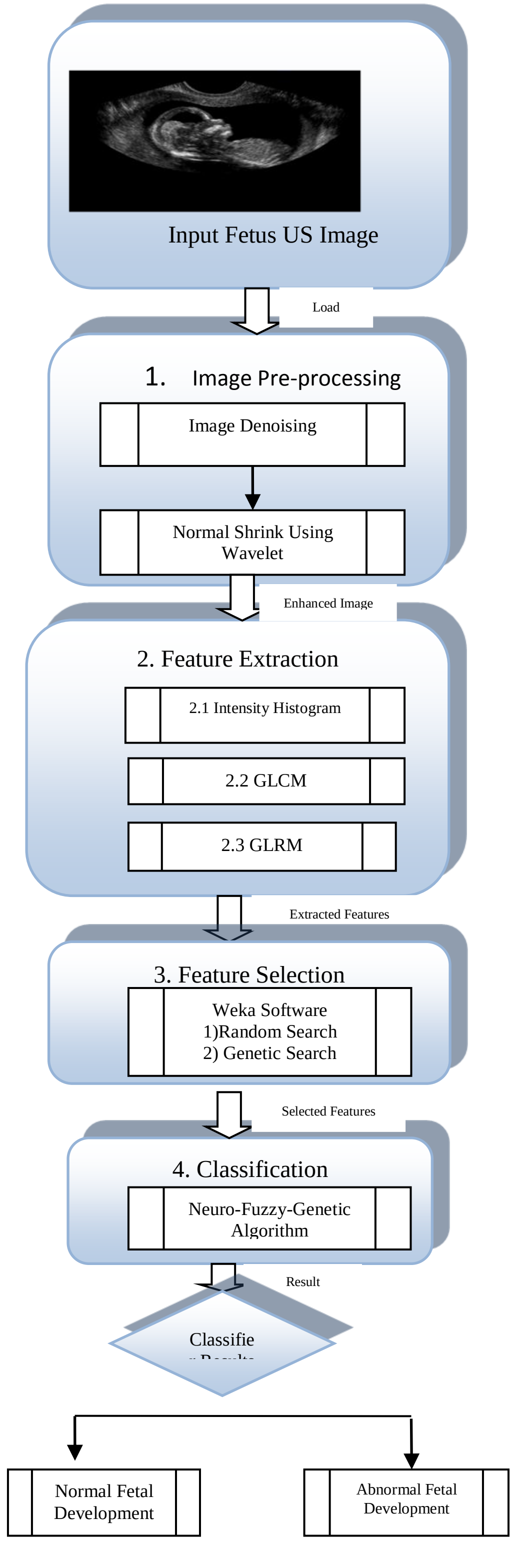

Figure 9: Proposed Methodology

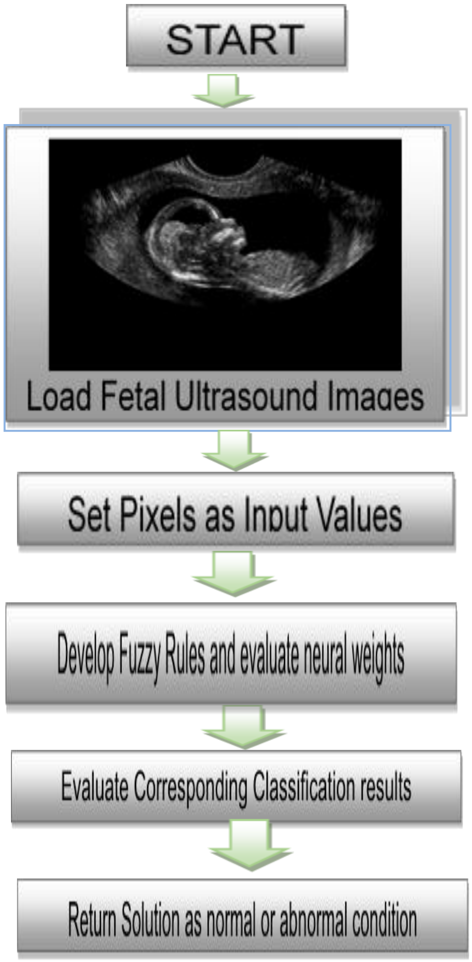

Figure 10: Workflow of implementation of neuro-fuzzy network

Steps

Step 1: Start the Algorithm.

Step 2: Load the ultrasound Image.

Step 3: Set image pixels as the input values to the algorithm.

Step 4: Develop the Fuzzy rules

Step 5: Evaluate the neural weights w(i) assigned the neurons.

Step 6: Evaluate the corresponding classification results

Step 7: Return the solution.

Step 9: Stop the Algorithm

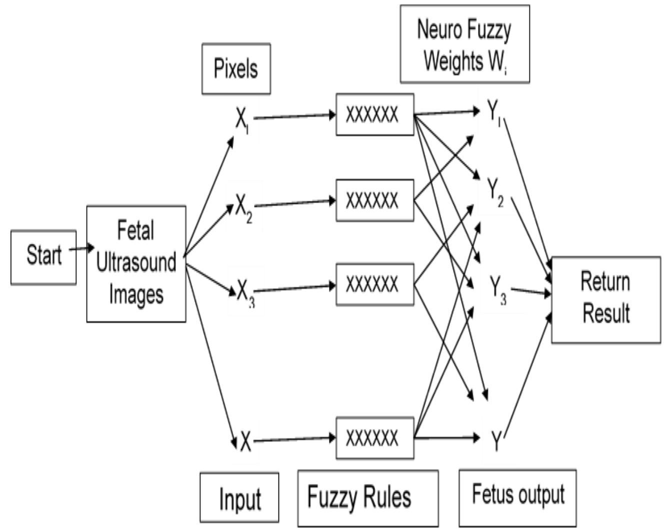

Figure 11: Training of the data set on the model adopted

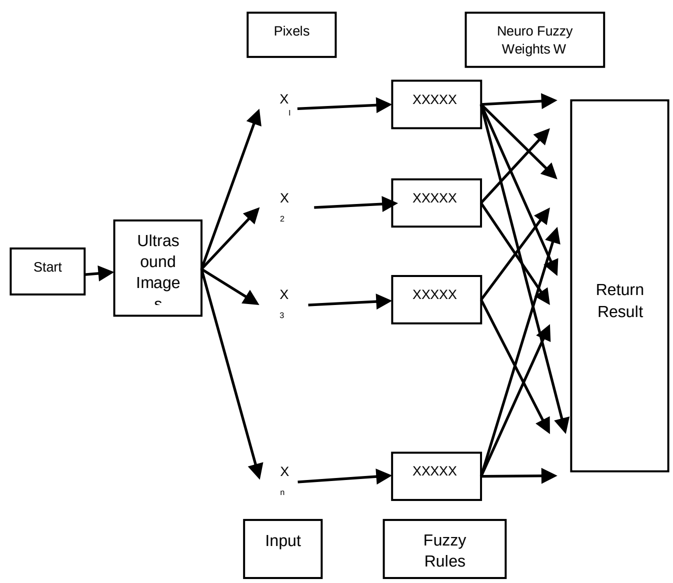

Fig. 12: Testing of the data set on the model adopted

V. RESULTS AND DISCUSSION

The findings within this study, containing preprocessing as well as features extraction are carried out using Matlab 15.0. The fetal development classification is carried out working with Weka. Four ultrasound images of human fetal were used to carry out the preprocessing and feature extraction. Then the input was the extracted features which results to perform the classification of fetal development. The proposed classification technique is compared with existing technique. The proposed system can easily identify the growth of fetal very accurately.

A. Comparison of the proposed method with existing technique

The proposed method works by using four fetal ultrasound images to obtain preprocessing results. The number as well as dimensions of each and every image differs from the others, still our method can effectively classify each image as abnormal and normal case. In the diagnosis of fetal development, the classification accuracy is more essential because the consequences of an inappropriate diagnosis can potentially result in health problems or even cause death. Table 4 shows the increase in average classification accuracy rates of different strategies. By utilizing only the shape features to differentiate fetal growth as normal or abnormal does not give classification accuracy more reliable. By integrating texture and shape characteristics, there is increase in accuracy drastically and by integrating intensity and texture-shape characteristics, maximum classification accuracy is achieved. The best rate of accuracy achieved during classification is 97% achieved through using the neuro-fuzzy method. Our technique has provided the maximum accuracy rate of classification so it is best appropriate for CAD. So as to completely verify the efficiency of proposed technique, specificity, precision, sensitivity, recall, F-measure of all the techniques are also computed according to the simulation results which are explained in Table 4. The values associated with sensitivity and specificity reveal one more way of the diagnosing accuracy that considers the variance in consequences of diagnostic. The performance of the system becomes better as the values of specificity and sensitivity becomes larger. Table 4 represents the values of sensitivity and specificity acquired using proposed technique which is larger among different methods. ROC curve is utilized for evaluating the accuracy which is shown in the Fig. 18 and listed in Table 4. The superiority of proposed method over the existing ones is proved.

Table4: Comparison Result

Existing classification Technique								
S. No	**Image name**	**Accuracy (%)**	**TP Rate (%)**	**FP Rate (%)**	**Precision (%)**	**Recall (%)**	**F-Measure (%)**	**ROC Area (%)**
1	Us_orig	85.38	0.853	0.073	0.898	0.853	0.846	0.89
2	Us1	89.30	0.893	0.053	0.907	0.893	0.892	0.92
3	Us2	86.7	0.867	0.067	0.879	0.867	0.865	0.9
4	Us3	89.3	0.893	0.053	0.919	0.893	0.891	0.92
Proposed Classification Technique								
S. NO	**Image name**	**Accuracy (%)**	**TP Rate (%)**	**FP Rate (%)**	**Precision (%)**	**Recall (%)**	**F-Measure (%)**	**ROC Area (%)**
1	Us_orig	97.30	0.973	0.013	0.975	0.973	0.973	0.999
2	Us1	90.70	0.907	0.047	0.917	0.907	0.906	0.99
3	Us2	93.3	0.933	0.033	0.934	0.933	0.933	0.994
4	Us3	94.7	0.947	0.027	0.947	0.947	0.947	0.995

B. Analysis of the proposed method and results of existing classifiers

The performance of the neuro-fuzzy was calculated by evaluating confusion matrix and the receiver operator characteristic curve (ROC). The result listed in Table 5 represents the comparison performance of the proposed technique with existing one. The proposed technique can extract the abnormal cases accurately and more effectively, giving information with minimized FP rates.

Table5: Comparison Classification results

Classifier Name	**Artificial Neural Network (%)**		**Neuro- Fuzzy using Genetic (%)**	
Correctly classified instances	90.6667 %	68	93.3333%	70
Incorrectly classified instances	9.3333%	7	6.6667 %	5

- **Assessment Measures**

Table 6: Confusion Matrix

Actual Class			
		Negative	Positive
Predicted Class	Negative	68	70
	Positive	7	5

This matrix illustrates the actual versus the predicted class in classification problems, where each column represents the instances in an actual class and rows represent the instances in a predicted class. True positives (TP) and true negatives (TN) shows the number of samples correctly classified in the positive and negative classes, while false positives (FP) and false negatives (FN) represent the number of misclassified positive and negative examples, respectively.

1. **Accuracy** represents how many predictions of the classifier were in fact correct, whereas the error rate is the percentage of misclassified examples in total. Nevertheless, the accuracy/error might not be appropriate performance measures for imbalanced datasets where the class priors are very different, because they will be strongly biased toward the majority class. The comparison in Figure 13 shows the accuracy of different images with the existing and the proposed technique.

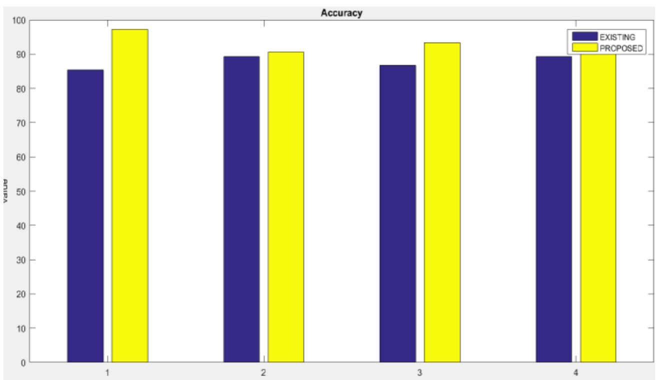

Figure 13: Comparison graph showing accuracy of testing dataset

2. **Recall** or sensitivity represents how many positive examples the classifier was able to correctly identify (in the recurrence problem this is the percentage of patients with recurrence identified as such). Figure 14 and Figure15 show the comparison between the existing and the proposed rate of sensitivity for different ultrasound images.

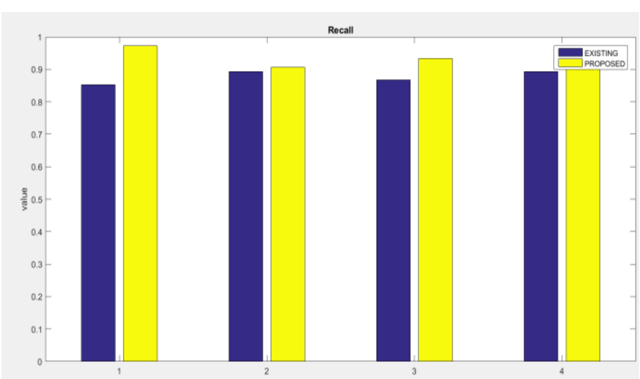

Fig. 14: Comparison graph depicting the recall

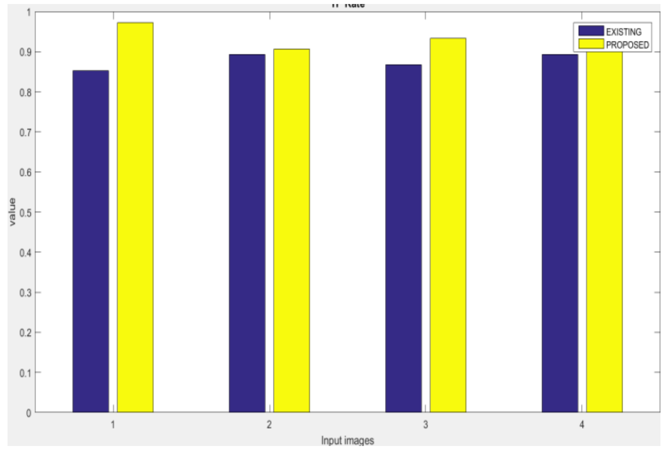

Figure15: Comparison graph depicting the TPR

3. **Specificity** represents how accurately the classifier behaves in terms of predicting the negative class (in the recurrence problem this is the percentage of patients without recurrence identified as such).

4. **Precision** shows the proportion of the correctly predicted positive cases relative to all the predicted positive ones (in the recurrence problem this is the percentage of patients identified as having recurrence that actually recur) in Figure16.

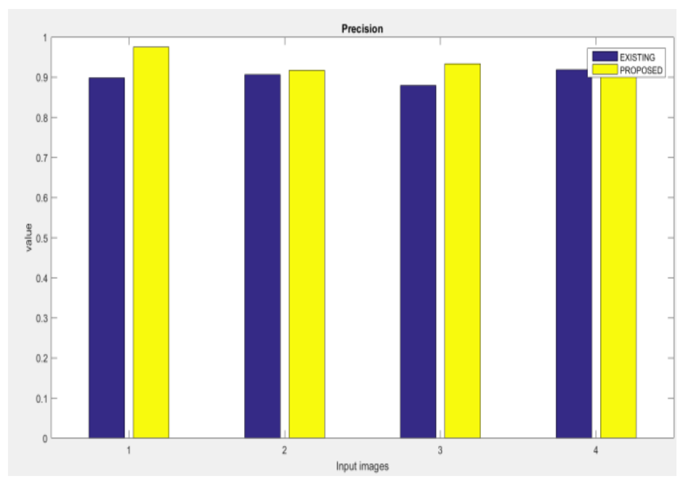

Figure16: Comparison graph depicting the Precision

5. **F-measure** is defined as the harmonic mean of precision and recall, providing a balance between both of them that better reflects the performance of a classifier in the presence of an underrepresented class. The comparison in Figure 17 shows the F-measure rate of the fetal ultrasound images.

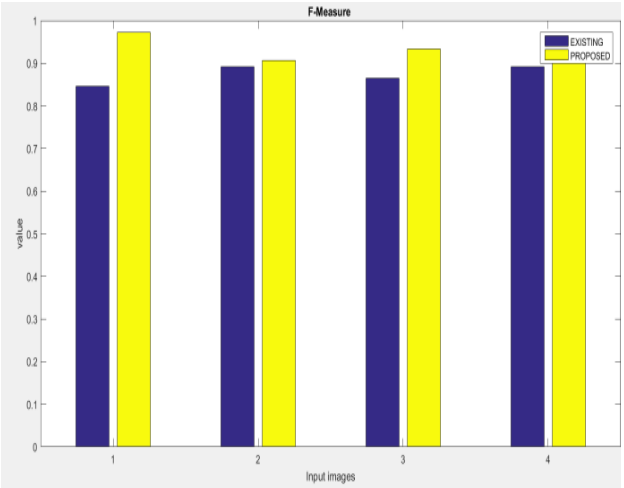

Figure 17: Comparison graph depicting the F-Measure

6. ROC Curve: The ROC curve is utilized in computing the predictive accuracy of the proposed model. This signifies the TPR as well as FPR. The region within the ROC curve called AUC categorized among the finest techniques for comparing classifiers within two issues. The test outcomes perform better when the ROC curve goes up rapidly in the direction of upper left corner of the graph else when the value of AUC is greater, Region near 1 demonstrates the reliable examination while region near 0.5 indicates the unreliable evaluation. Figure18 shows the ROC curve of the techniques compared.

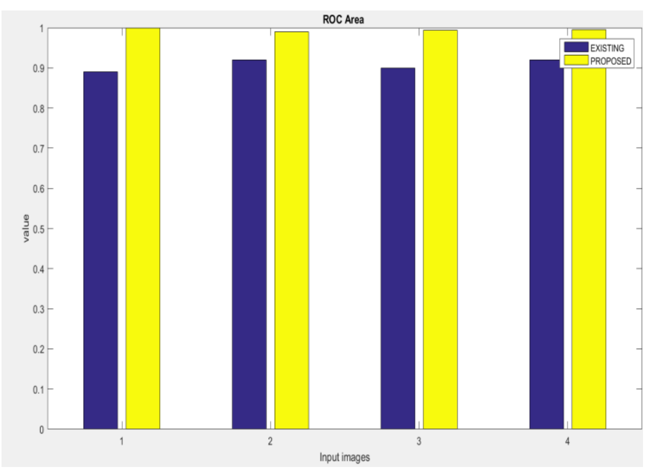

Figure 18: Comparison graph depicting the ROC Area

7. Fall Out or False Positive rate is defined as probability of falsely rejecting the null hypothesis for a particular test. Figure19 shows the percentage of falsely rejected samples by the existing and the proposed technique.

The appealing outcomes must be because of both the precise preprocessing and segmentation method as well as the efficient classification technique. Initially in image pre-processing, the cropping and the edge detection method improves the boundary contrast detecting the object rather than interferential layers, thereby enhancing the accuracy of preprocessing and laying down the feature extraction foundation. Neuro-fuzzy is employed for overcoming the existing classifiers producing more accurate results of classification, and this is because of random processing decreasing the correlation among distinctive learners in the ensemble and the variance reduction by averaging over learners. Therefore best results of performance describe our proposed technique as best for distinguishing between normal and abnormal cases of fetal growth effectively.

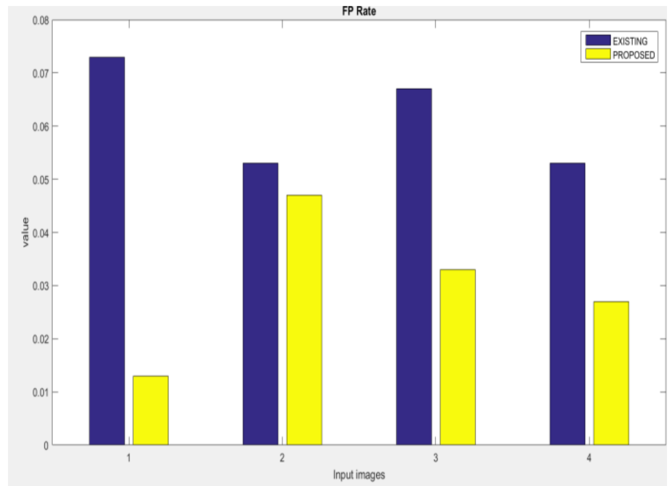

Figure 19: Comparison graph depicting the FPR

VI. Conclusion and Future Scope

In this study, the different classifier has been investigated for diagnosing the fetal development measurements. The accuracy of the classifier was predicted on the basis of the feature selection, training samples selected and the classifiers ability to learn from the training samples. The main objective is to find the better classifier for fetal diagnosis which is achieved in the results. The proposed result show that neuro-fuzzy using genetic algorithm proved to be more accurate and efficient as compared to ANN which gives approximately 97% accuracy in training as well as testing. In near future, the evaluation of multiple feature extraction techniques which will provide more accurate classification result is to be achieved on live dataset.

References

[1]. P. Loughna, "*Fetal size and dating: charts recommended for clinical obstetric practice Ultrasound", Ultrasound*, Vol. 17, No 3, pp.160-166, 2009.

[2]. B. Hearn-Stebbins, "*Normal fetal growth assessment: A review of literature and current practice*" Journal of

Diagnostic Medical Sonography, Vol. 11, No. 4, pp. 176-187, 1995.

[3]. Pramanik, Manojit, M. Gupta, K. B. Krishnan, "*Enhancing reproducibility of ultrasonic measurements by new users.*" SPIE Medical Imaging International Society for Optics and Photonics, India, pp.6-12, 2013.

[4]. Carneiro Gustavo, "*Knowledge-based automated fetal biometrics using syngo Auto OB measurements*", Siemens Medical Solutions, Vol. 6, Issue.7, pp.1-6, 2008.

[5]. J. Espinoza, "*Does the use of automated fetal biometry improve clinical work flow efficiency"*, Journal of Ultrasound in Medicine, Vol. 32, No. 5, pp.847-850, 2013.

[6]. H. Sujana, S. Swarnamani, "*Application of Artificial Neural Networks for the classification of liver lesions by texture parameters*", Ultrasound in Med. and Biol., Vol.22, No.9, pp. 1177- 1181, 1996.

[7]. H. Yoshida, D. Casalino "*Wavelet packet based texture analysis for diferentiation between benign and malignant liver tumors in ultrasound images*", Phys in Med and Biol, Vol. 48, Issue.22, pp. 3735-3753, 2003.

[8]. T. Chikui, K. Yoshiura, "*Sonographic texture characterization of salivary gland tumors by fractal analysis*", Ultrasound in Med. and Biol., Vol. 31, No.10, pp.1297-1304, 2005.

[9]. J. Minuillon, A. Rosemary Tate, *"Classifier combination for in vivo magnetic resonance spectra of brain tumors",* Lecture Notes in Computer Science (LNCS 2364), Berlin, pp. 282-292, 2002

[10]. S. Ramaswamy, P. Tamayo, "*Multiclass cancer diagnosis using gene expression signatures",* PNAS, Vol. 98, No. 26, pp. 15149-15154, 2001.

[11]. X. Chen, "*Multi-class feature selection for texture classification*", Pattern Recognition Letters, Vol. 27, Issue.14, pp. 1685-1691, 2006.

[12]. A. Philippe, T. Boudier, "*Adaptive active contours (snakes) for the segmentation of complex structures in biological images*", Image J Conference, India, pp.34-41, 2006.

[13]. Haralick, M. Robert , "*Statistical and structural approaches to texture*", Proceedings of the IEEE, Vol.67,No.5, pp.786-804, 1979.

[14]. S. Selvarajah, S.R. Kodituwakku, "*Analysis and comparison of texture features for content based image retrieval*", International Journal of Latest Trends in Computing, Vol. 2, No.1, pp.108-113, 2011.

[15]. S. Poonguzhali, G. Ravindran, "*Automatic classification of focal lesions in ultrasound liver images using combined texture features*", Information Technology Journal, Vol. 7, No. 1, pp: 205-209, 2008.

[16]. Pietikainen, Matti, T. Ojala, and X. Zelin, "*Rotation-invariant texture classification using feature distributions",* Pattern Recognition, Vol. 33 , No. 1, pp.43-52, 2000.

[17]. J. Flusser, T. Suk, "*Rotation moment invariants for recognition of symmetric objects*", IEEE Transactions on Image Processing, Vol. 15, No. 12, pp. 3784-3790, 2006.

[18]. B.F. Branstetter, "*Basics of Imaging Informatics: Part1", Radiology*, Vol. 243, Issue.7, , pp. 656-667, 2007.

[19]. N. Sharma, A. Bajpai, R. Litoriya, "*Comparison the various clustering algorithms of weka tools facilities",* Vol. 4, No.7, pp.1-6, 2012.

[20]. I. A. Basheer, M. Hajmeer, "*Artificial neural networks: fundamentals, computing, design, and application*", Journal of microbiological methods, Vol. 43, No. 1, pp. 3-31, 2000.

[21]. O. Marques, "*Practical image and video processing using MATLAB*", John Wiley & Sons, Singapore, pp.1-696, 2011.

[22]. S. Gupta, R.C. Chauhan S.C. Saxena, "*Locally adaptive wavelet domain Bayesian Processor for denoising medical ultrasound images using speckle modelling based on Rayleigh distribution"*, IEEE Poc.-Vis. Image Signal Process.,Vol.152,No.1, pp. 129-35, 2005.

[23]. S. Gupta, L. Kaur, R.C. Chauhan, S.C. Saxena, *"A wavelet based Statistical Approach for Speckle Reduction in Medical Ultrasound Images"*, Medical and Biological Engineering and computing, Vol.42, Issue.2, pp.189-192, 2004.

[24]. S.Gupta, L.Kaur, R.C.Chauhan, S.C.Saxena, *"A versatile technique for visual enhancement of medical ultrasound images"*, Digital signals Processing, Vol. 17, Issue.3, pp.542-560, 2007.

[25]. L. Kaur, S. Gupta, R.C.Chauhan, "*Image denoising using Wavelet Thresholding"*, InICVGIP, Vol.2, pp.16-18, 2002.

[26]. A. Ray, B. Kartikeyan, S. Garg, "*Towards Deriving an Optimal Approach for Denoising of RISAT-1 SAR Data Using Wavelet Transform*", International Journal of Computer Sciences and Engineering, Vol.4, Issue.10, pp.33-46, 2016.

[27]. S. Arivazhagan, S. Deivalakshmi, K. Kannan, B.N. Gajbhiye, C.Muralidhar, Sijo N Lukose, M.P. Subramanian, "*Performance Analysis of Wavelet Filters for Image Denoising*", Advances in Computational Sciences And Technology, Vol.1, No.1, pp.1-10,2007.

[28]. M. Fernandes, "*Data Mining: A Comparative Study of its Various Techniques and its Process*", International Journal of Scientific Research in Computer Science and Engineering, Vol. 5 ,No. 1, pp.19-23, 2017.

Authors Profile

P. Kaur is an Assistant Professor in the Department of Computer Engineering & Technology at Guru Nanak Dev University, Amritsar. She is pursuing Ph. D. from Guru Nanak Dev University, Amritsar. Her research interests include Image Processing and Genetic Algorithm.

Dr. G. Singh is Professor, Department of Computer Science at Guru Nanak Dev University Amritsar, India. Major Research interest includes Cloud Computing and Distributed Processing. Already Published 100 Research paper in International and National journals & Conferences.

Dr. P Kaur is an Assistant Professor in the Department of Computer Science at Guru Nanak Dev University Amritsar, India. She has completed her Ph. D. from Guru Nanak Dev University, Amritsar in the year 2011. Her research interests include Software Engineering, Web Security, Web Usability, Open Source Software and Service-oriented Architecture. She has around 45 publications in different International/National Journals as well as Conferences.